Metals in Medicine

β-Diketonate versus β-Ketoiminate: The Importance of a Ferrocenyl Moiety in Improving the Anticancer Potency

Matthew Allison,[a] Daniel Wilson,[a] Christopher M. Pask,[a] Patrick C. McGowan,*[a] and Rianne M. Lord*[b, c]

Herein we present a library of fully characterized β-diketonate and β-ketoiminate compounds that are functionalized with a ferrocenyl moiety. Their cytotoxic potential has been determined by screening against human breast adenocarcinomas (MCF-7 and MDA-MB-231), human colorectal carcinoma *p53* wild type (HCT116 $p53^{+/+}$) and normal human prostate (PNT2) cell lines. The ferrocenyl β-diketonate compounds are more than 18 times more cytotoxic than the ferrocenyl β-ketoiminate analogues. Against MCF-7, compounds functionalized at the *meta* position are up to nine times more cytotoxic than when functionalized at the *para* position. The ferrocenyl β-diketonate compounds have increased selectivity towards MCF-7 and MDA-MB-231, with several complexes having selectivity index (SI) values that are more than nine times (MCF-7) and more than six times (MDA-MB-231) that of carboplatin. The stability of these compounds in dimethyl sulfoxide (DMSO) and dimethylformamide (DMF) has been assessed by NMR spectroscopy and mass spectrometry studies, and the compounds show no oxidation of the iron center from Fe^{II} to Fe^{III}. Cytotoxicity screening was performed in both DMSO and DMF, with no significant differences observedin their potency.

Cisplatin, *cis*-$[Pt(NH_3)_2Cl_2]$,[1] is the best-known metal-based compound widely used in the clinic for the treatment of cancer.[2,3] Since its success, a variety of platinum-based therapeutics have been designed and tested,[4,5] however, alternatives are being developed due to tumors developing platinum resistance, which have rendered the platinum-based drugs ineffective. Due to the inability of the platinum compounds to target the cancerous cells over normal cells, high levels of toxicity are observed, leading to severe side-effects such as nephrotoxicity.[6] There has been a surge in research towards different metal-based therapeutics,[7–11] including organometallic compounds. Ferrocenyl compounds derived from tamoxifen, are known as ferrocifens, and are amongst the earliest organometallic selective estrogen receptor modulators (SERM).[12,13] Ferrocenyl hydroxytamoxifen (Fc-OH-Tam, Figure 1A)[14] is one of the leading compounds of this class, and possesses anti-proliferation against both hormone-dependent (MCF-7) and hormone-independent (MDA-MB-231) breast cancer cells. Additionally, Fc-OH-Tam, has been shown to significantly inhibit *in vivo* growth of MDA-MB-231 xenografted tumors in mice when formulated in lipid nanocapsules (LNCs).[15,16] The dual effect of targeting both MCF-7 and MDA-MB-231 is very significant, since the organic compound hydroxytamoxifen (OH-Tam) shows activity against MCF-7 only. This highlights the importance the ferrocenyl moiety on the increased activity against breast cancers.[17]

Although the mechanism of action is still not fully understood, it was found that such Fc-OH-Tam compounds can generate hydroxyl radicals in physiological solutions, and this Fenton-type reaction is thought to lead to DNA damage by radicals.[17,18] Since this discovery, there have been many ferrocenyl derived compounds which have been synthesized and screened for their cellular activities.[19–22] It was also shown that Fc-OH-Tam can induce strong senescence in MDA-MB-231 cells and exhibits low apoptosis.[23] Electron transfer processes between the ferrocenyl and ferrocenium states are fast and reversible, and the ferrocenyl moiety will exist as a mixture of the neutral ferrocenyl and cationic radical ferrocenium species.[24–26] It was therefore suggested that such compounds can be administered in either the reduced ferrocenyl or

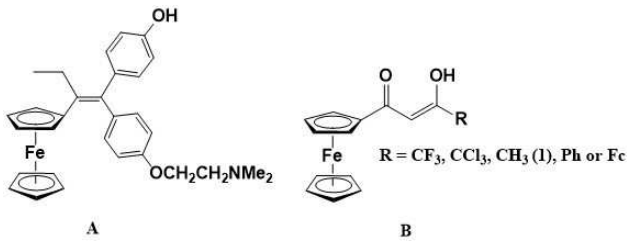

Figure 1. Chemical structures of A) ferrocenyl hydroxytamoxifen[14] and B) ferrocenyl β-diketonates.[30]

[a] Dr. M. Allison, D. Wilson, Dr. C. M. Pask, Prof. P. C. McGowan
School of Chemistry, University of Leeds
Leeds, LS2 9JT (UK)
E-mail: p.c.mcgowan@leeds.ac.uk
[b] Dr. R. M. Lord
School of Chemistry, University of East Anglia, Norwich Research Park, Norwich NR4 7TJ (UK)
E-mail: r.lord@uea.ac.uk
[c] Dr. R. M. Lord
School of Chemistry and Biosciences, University of Bradford
Bradford, BD7 1DP (UK)

Supporting information for this article is available on the WWW under https://doi.org/10.1002/cbic.202000028

Metals in Medicine *This article is part of a Special Collection dedicated to the Metals in Medicine Workshop in Paris, France, 2019. To view the complete collection, visit our homepage*

oxidized ferrocenium state, providing the formal reduction potential of the ferrocenyl group is low enough to allow ferrocenyl oxidation inside a cell. Many researchers have shown that this oxidation from Fe^{II} to Fe^{III} can cause the compounds to undergo chemical oxidation to give quinone methides (QM)[27,28] which were able to strongly inhibit *in vitro* thioredoxin reductase (TrxR).[28,29]

Swarts and co-workers developed and screened ferrocenyl β-diketonates, and also provided evidence that halides had a significant effect on the compound's cytotoxicity (Figure 1B).[30] The compound functionalized with a CF_3 moiety exhibited low μM activity against colorectal adenocarcinoma (CoLo 320DM), and was more cytotoxic than cisplatin. We have previously synthesized a range of β-diketonate and β-ketoiminate ligands, which we have used for complexation reactions with metals such as Ti, Ru and Ir.[31–33] However, the ligands exhibit no toxicity, with IC_{50} values >100 μM. Herein, we have functionalized these ligands with ferrocenyl and extended the library published by Swarts et al. (Figure 1B). We report an increase in cytotoxicity against human carcinomas, highlighting the ferrocenyl β-diketonate ligands to be more cytotoxic than the ferrocenyl β-ketoiminate analogues. The stability of these compounds has been assessed by NMR and mass spectroscopy in DMSO and DMF over 4 days, showing no oxidation of the iron centers, but the possibility of new species in solution.

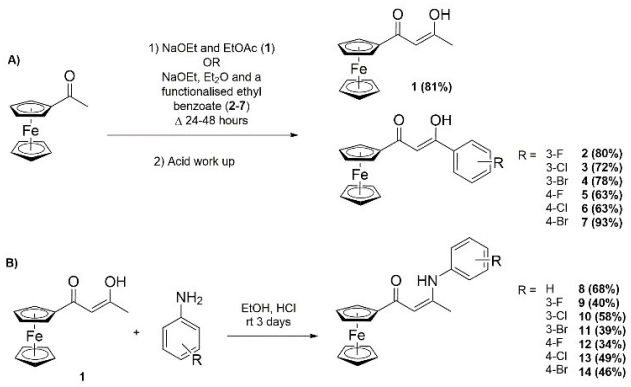

Scheme 1. Synthesis of A) ferrocenyl β-diketonate compounds **1**–**7** and B) ferrocenyl β-ketoiminate compounds **8**–**14**.

Additionally, the compounds were screened against a colorectal carcinoma cell line, HCT116 $p53^{+/+}$, after being dissolved in DMF. The results are similar to those obtained in DMSO, unlike the clinical platinum compounds, where carboplatin and oxaliplatin become less cytotoxic in DMF.

A simple acid-catalyzed Friedel-Crafts acylation was used to synthesize acetyl ferrocene, which was purified by column chromatography, followed by a Claisen condensation with a functionalized acetophenone (1 eq.). Compound **1** was synthesized by refluxing acetyl ferrocene (1 eq.), sodium ethoxide (2 eq.) and ethyl acetate for 3 hours. After an acid work up and recrystallization from hexane, red crystals were obtained in an 81% yield (Scheme 1A). Complexes **2**–**7** were synthesized by refluxing acetyl ferrocene (1 eq.), sodium ethoxide (1 eq.) and a functionalized ethyl benzoate (1 eq.) in diethyl ether for 3 hours (Scheme 1A). These compounds were purified by column chromatography and obtained in yields of 63–93%. Compounds **8**–**14** were synthesized by addition of compound **1** (1 eq.), to a functionalized aniline (excess) and a catalytic amount of concentrated hydrochloric acid. The reaction mixture was stirred at room temperature for 3 days, and after removal of the solvent and purification, the compounds were obtained in 34–68% yields (Scheme 1B). All compounds were fully characterized by ^{1}H NMR and $^{13}C\{^{1}H\}$ NMR spectroscopy, elemental analysis, high resolution mass spectrometry and single crystal X-ray diffraction where possible.

Crystal structures of compounds **1**–**13** are reported herein, and the crystal structure of compound **14** has previously been published.[34] Red/orange single crystals suitable for X-ray crystallographic analysis were obtained for compounds **1**–**7**, by slow evaporation of an acetonitrile solution (Figure 2). Compound **1** has previously been published, however, this is the first time a crystal structure has been obtained. The compounds all crystallized in either an orthorhombic or monoclinic cell, and structures were solved in space groups $P2_12_12_1$ (**1**), $P2_1/n$ (**2**, **6**, **7**), C_2/c (**3**, **4**) or $P2_1/c$ (**5**). The cyclopentadienyl (Cp) substituents of the ferrocenyl adopt an eclipsed conformation in all cases, with the exception of compound **7**, which has a disordered staggered Cp rings. The eclipsed arrangement has been postulated to be the energetically preferred conformer.[35,36] The β-diketonate section of the compounds are all planar, with

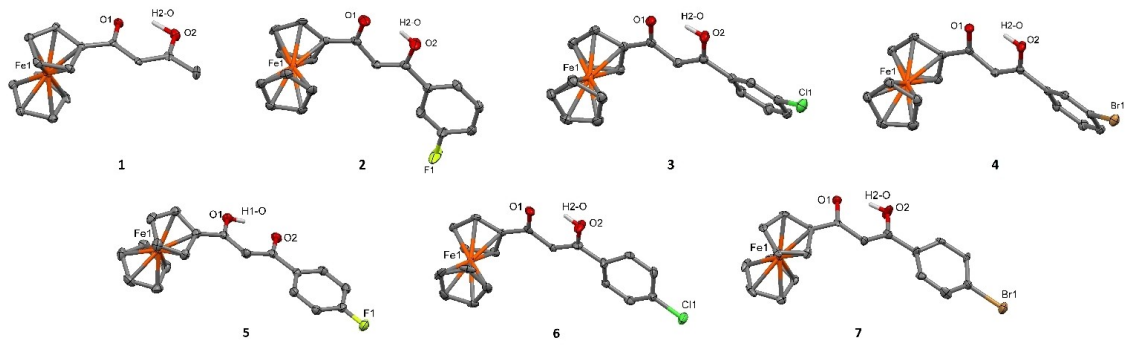

Figure 2. Molecular structures of ferrocenyl β-diketonate compounds **1**–**7**. Displacement ellipsoids are at the 50% probability level, and hydrogen atoms and disordered atoms are omitted for clarity.

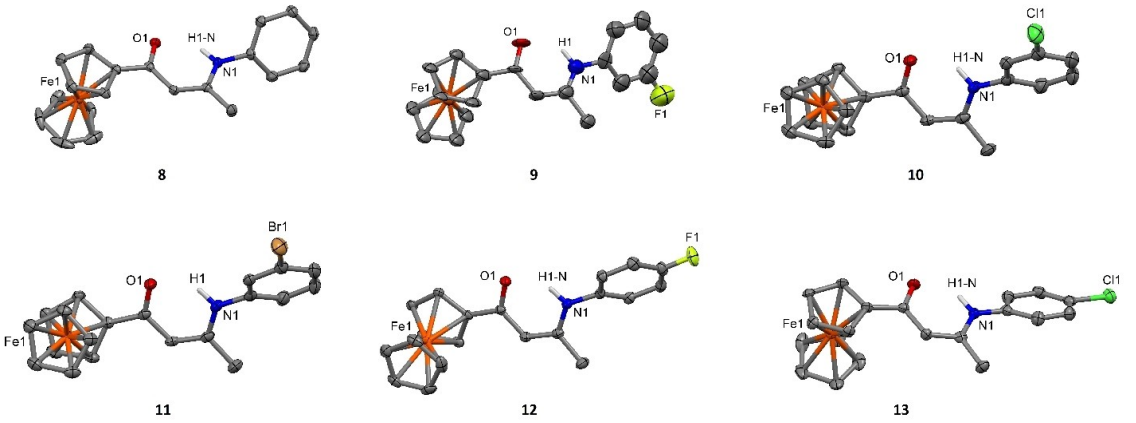

Figure 3. Molecular structures of ferrocenyl β-diketonate compounds **8**–**13**. Displacement ellipsoids are at the 50% probability level, and hydrogen atoms and disordered atoms are omitted for clarity.

O1–C11–C12–O2 angles of 119–122° (Table S3) and carbonyl bond lengths of 1.2–1.3 Å (Table 1). Short intramolecular hydrogen bonding interactions are observed between O(1)-H···O(2), at a distance of 2.4–2.5 Å (D···A) in all cases, which is characteristic for such acetylacetone molecules in their enol formation.

Red/orange singles crystals suitable for X-ray crystallographic analysis were obtained for compounds **8**–**13**, by slow cooling from hot ethanol then storing at −20 °C or by slow evaporation from acetone (Figure 3). The compounds crystallized in either a monoclinic or orthorhombic cell, and structures were solved in the space group $P2_1/c$ (**8**, **10**, **11** and **13**), $P2_1/n$ (**12**), or $Pca2_1$ (**9**). In the case of the β-ketoiminate compounds, the Cp moiety adopts an eclipsed conformation in all cases. As with the previous compounds, compound **8**–**13** have short intramolecular hydrogen bonding, with O1···H–N1 distances of 2.5–2.6 Å (D···A). All crystallographic data are stated in Table S1a–b (1–7) and Table S2a–b (8–13).

The ferrocenyl β-diketonate compounds are distinguishable by the presence of the methine singlet at ~5.5–6.5 ppm, and in some solvents the appearance of the OH resonance at ~16.0 ppm. Upon synthesis of the ferrocenyl β-ketoiminate compounds, the methine resonances undergo a minor shift and the disappearance of the OH resonance, with the appearance of a new aniline NH resonance at 11–13 ppm verifying the successful synthesis. NMR samples were first prepared in $CDCl_3$, however, broad resonances were observed (Figure 4, blue). This was attributed partly to the fluctuating nature of the ligands, as they can undergo tautomerisation between the cyclic enol and diketo forms.[37–39] The use of more polar solvents, that is [D_3] acetonitrile, stabilized the enol system through hydrogen bonding interactions, producing sharp resonances in the NMR spectra (Figure 3, green).

To address the stability of these compounds prior to cell screening, ^{1}H NMR spectroscopy was used to monitor any changes in the compounds, and the unfunctionalized ferrocenyl β-diketonate compound **1** and unfunctionalized ferrocenyl β-ketoiminate compound **8** were used in this study. The compounds (5 mg) were dissolved in [D_6]DMSO and an initial spectrum taken, and then recorded at varying time intervals between initial and 4 days. Selected time intervals are shown for compounds **1** and **8**, in Figures 5 and 6, respectively. Both of the compounds show the appearance of new resonances which are also similar to those observed in the 4 day NMR spectra of

Table 1. Selected bond lengths for ferrocenyl β-diketonate compounds **1**–**7** and ferrocenyl β-ketoiminate compounds **8**–**13**.

Cmpd	Bond lengths [Å] C11–O1	C11–C12	C12–C13	C13–O2 or C13–N1
1	1.284(6)	1.412(8)	1.371(8)	1.320(7)
2	1.266(3)	1.449(4)	1.366(4)	1.331(3)
3	1.260(5)	1.441(5)	1.363(5)	1.329(5)
4	1.262(2)	1.437(3)	1.358(3)	1.334(2)
5	1.302(2)	1.397(3)	1.400(3)	1.294(2)
6	1.274(7)	1.433(8)	1.355(8)	1.332(7)
7	1.276(9)	1.425(10)	1.359(11)	1.320(10)
8	1.2560(18)	1.433(2)	1.373(2)	1.3561(10
9	1.25(5)/ 1.25(4)	1.29(5)/ 1.56(5)	1.35(6)/ 1.30(6)	1.34(6)/ 1.32(5)
10	1.258(2)	1.429(3)	1.372(3)	1.346(3)
11	1.260(3)	1.425(3)	1.378(4)	1.341(3)
12	1.24(5)/ 1.20(4)	1.44(5)/ 1.47(6)	1.37(7)/ 1.35(6)	1.29(6)/ 1.36(5)
13	1.267(5)	1.438(5)	1.374(6)	1.358(5)

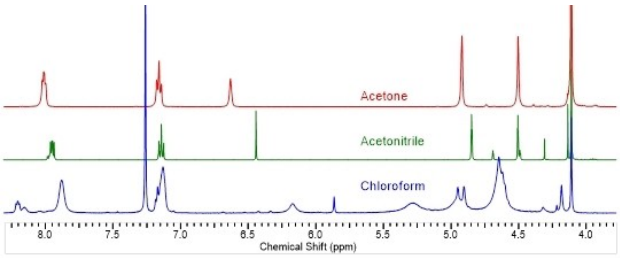

Figure 4. ^{1}H NMR spectra (400 MHz, 298 K) of unfunctionalized ferrocenyl β-diketonate compound **1** in $CDCl_3$ (blue), [D_3]acetonitrile (green) and [D_6] acetone (red).

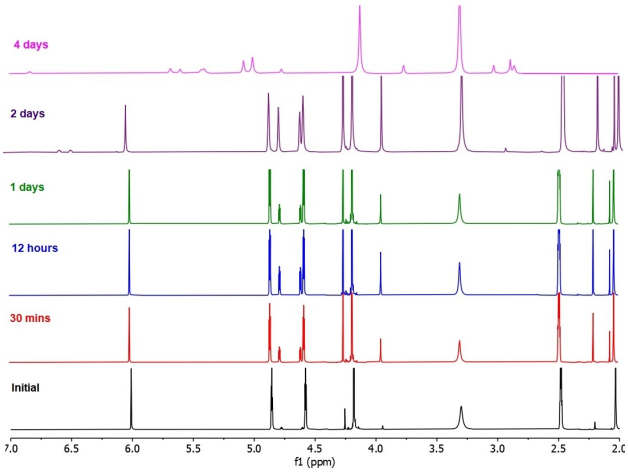

Figure 5. ^{1}H NMR spectra (298 K, 400 MHz) of ferrocenyl β-diketonate compound **1** in DMSO at selected time intervals from initial to 4 days.

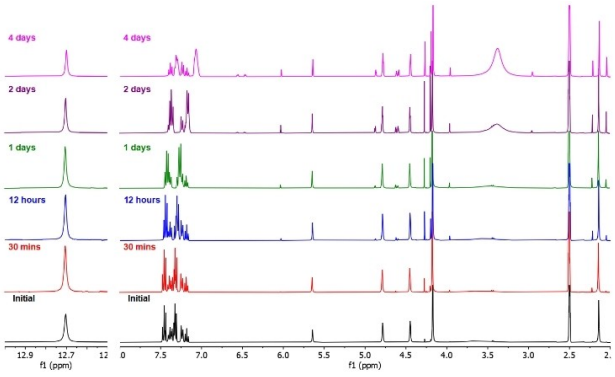

Figure 6. ^{1}H NMR spectra (298 K, 400 MHz) of ferrocenyl β-ketoiminate compound **8** in DMSO at selected time intervals from initial to 4 days.

acetyl ferrocene (Figures S1 and S2, respectively), showing there is likely some rearrangement of the compounds in solution, but no decomposition to acetyl ferrocene or ferrocene. Although the solutions turn darker in color over time (Figures S5 and S6), the NMR spectra do not broaden and there is no evidence of paramagnetic resonances, indicating no oxidation from Fe^{II} to Fe^{III}.

The stability of compounds **1** and **8** were also assess by dissolving 5 mg in [D_7]DMF and ^{1}H NMR spectra recorded at the same time intervals as previously discussed. Although DMF solutions of compound **1** appear to darken over 2 hours (Figure S5), the spectra showed no significant changes until day 4. In comparison, compound **8** exhibited significant changes in the aromatic region (7.0–7.5 ppm) after only 30 mins, unlike the studies in DMSO, which shows the compound changing slowly over time (Figures 6 and S4). These changes were surprising, as compound **8** did not experience darkening of the solution when dissolved in DMF for 2 hours (Figure S6). As with the DMSO results, the NMR spectra in DMF do not broaden and there is again no evidence of paramagnetic resonances, indicating no oxidation from Fe^{II} to Fe^{III}. In attempts to establish the structures in solution, mass spectrometry was performed after samples were dissolved in DMSO or DMF over a period of 4 days. Although there is evidence of each compound in solution over time, there are multiple new mass peaks which could not be assigned to known species, and we were unable to elucidate the structures or rearrangement products of these compounds in solution (Table S4).

The range of compounds were screened for their cytotoxicity against human breast adenocarcinomas MCF-7 and MDA-MB-231, and human colorectal carcinoma *p53* wild type, HCT116 $p53^{+/+}$ cell lines. Stock solutions in DMSO (100 mM) were made fresh on each day of testing, and were immediately ($<$5 mins) plated with the cell lines for 96 h (DMSO $<$0.1% v/v) before performing an MTT assay. The clinical drugs cisplatin (CDDP), oxaliplatin (OXA) and carboplatin (CARB) were screened for comparison. The results are shown in Table 2 and Figure 7, and across all of the cell lines tested, there is a general trend whereby the ferrocenyl β-diketonate compounds **1**–**7** are more cytotoxic than the analogous ferrocenyl β-ketoiminate compounds **8**–**14**. The most significant differences are observed against the triple negative breast adenocarcinoma, MDA-MD-231, where the ferrocenyl β-diketonate compounds are $>$18 times more cytotoxic than the ferrocenyl β-ketoiminate compounds (**6** *cf.* **13**, see Figure S7). In comparison, this is contrary to our previously investigated Ru^{II} and Ir^{III} complexes, in which the β-ketoiminate complexes were more cytotoxic than those with a β-diketonate ligand, where the latter were generally nontoxic.[31–33]

The unfunctionalized ferrocenyl β-diketonate compound **1** is moderately cytotoxic towards all cell lines, and generally the toxicity increases when the compound is functionalized with a halide substituent. Compounds **2**–**4** have a halide in the *meta* position of the arene ring, and the 3′-F (**2**) position has increased cytotoxicity when compared to 3′-Cl (**3**) and 3′-Br (**4**), following the order **2** $>$ **3** $>$ **4**. When using the same substituents in the *para* position (**5**–**7**), the activity is generally reversed and the 4′-Br compound **7** is more cytotoxic than the 4′-F (**5**) and 4′-

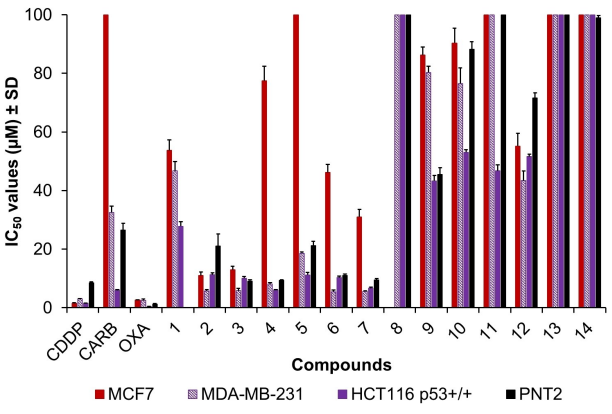

Figure 7. Bar-chart of IC_{50} values against MCF7, MDA-MB-231, HCT116 $p53^{+/+}$ and PNT2 for cisplatin (CDDP), carboplatin (CARB), oxaliplatin (OXA), ferrocenyl β-ketoiminate compounds **1**–**7**, and ferrocenyl β-ketoiminate compounds **8**–**14**.

Table 2. IC_{50} values [μM] ± SD after 96 h incubation with MCF-7, MDA-MD-231, HCT116 $p53^{+/+}$, and PNT2. All values are averages of duplicate of triplicate repeats. The values in parentheses are the selectivity index (SI) values, when compared to the normal cell lines PNT2.

Compound	IC_{50} values [μM] ± SD				
	MCF-7	MDA-MB-231	HCT116 $p53^{+/+}$ DMSO	HCT116 $p53^{+/+}$ DMF	PNT2
CDDP	1.5 ± 0.2 (5.7)	3.07 ± 0.02 (2.8)	1.5 ± 0.1 (5.7)	2.3 ± 0.1	8.5 ± 0.4
CARB	> 100 (< 0.27[a])	33 ± 2 (0.8)	6.0 ± 0.2 (4.5)	45 ± 2	27 ± 2
OXA	2.6 ± 0.2 (0.5)	2.6 ± 0.4 (0.5)	0.445 ± 0.002 (2.9)	1.6 ± 0.1	1.3 ± 0.2
1	54 ± 4 (1.9)	47 ± 3 (2.1)	28 ± 1 (3.6)	32 ± 1	> 100
2	11 ± 1 (1.9)	5.7 ± 0.5 (3.7)	11.3 ± 0.7 (1.9)	9.3 ± 0.4	21 ± 4
3	13 ± 1 (0.7)	5.8 ± 0.9 (1.6)	10.1 ± 0.5 (0.9)	5.8 ± 0.2	9.0 ± 0.5
4	77 ± 5 (0.1)	8.1 ± 0.4 (1.2)	6.0 ± 0.2 (1.6)	4.45 ± 0.09	9.4 ± 0.1
5	> 100 (< 0.2[a])	18.6 ± 0.5 (1.1)	11.2 ± 0.9 (1.9)	10.7 ± 0.6	21 ± 2
6	46 ± 3 (0.2)	5.4 ± 0.6 (2.1)	10.3 ± 0.6 (1.1)	4.8 ± 0.6	11.1 ± 0.4
7	31 ± 3 (0.3)	5.6 ± 0.2 (1.7)	6.7 ± 0.4 (1.4)	5.6 ± 0.5	9.4 ± 0.6
8	> 100 (n.d.)	> 100 (n.d.)	> 100 (n.d.)	59 ± 2	> 100
9	86 ± 3 (0.5)	80 ± 2 (0.6)	43 ± 2 (1.1)	52 ± 2	46 ± 2
10	90 ± 5 (1.0)	77 ± 5 (1.1)	53.1 ± 0.9 (1.7)	43 ± 2	88 ± 3
11	> 100 (n.d.)	> 100 (n.d.)	47 ± 2 (> 2.1[a])	41 ± 2	> 100
12	55 ± 4 (1.3)	43 ± 3 (1.7)	51.6 ± 0.7 (1.4)	56 ± 2	72 ± 2
13	> 100 (n.d.)	> 100 (n.d.)	> 100 (n.d.)	86 ± 2	> 100
14	> 100 (< 1.0[a])	> 100 (< 1.0[a])	> 100 (< 1.0[a])	84 ± 2	99 ± 1

[a] denotes the minimum SI value, as at least one of the IC_{50} values is > 100 μM n.d. denotes the values which cannot be determined, as both of the IC_{50} values are > 100 μM

CI (**6**), following the order **7** > **6** > **5**. This highlights the importance of the position of the halide substituent on the compound's *in vitro* activity, and the *meta* substituted compounds are up to 9 times more cytotoxic than the *para* substituted compounds against MCF-7 (**2** *cf.* **5**). The ferrocenyl β-diketonate compounds have an increased sensitivity towards the MDA-MD-231 cell line, with compounds **2**, **3**, **5** and **7** having IC_{50} values ranging from 5.4–5.8 μM . They have comparable activity to CDDP ($p > 0.05$) and are > 5 times more cytotoxic than CARB ($p < 0.05$).

The unfunctionalized ferrocenyl β-ketoiminate compound **8** is nontoxic against all cell lines (IC_{50} > 100 μM), and is up to 3.5 times less cytotoxic than the analogues β-diketonate compound **1** (HCT116 $p53^{+/+}$). There are no general trends observed when these compounds are functionalized in the *meta* position of the aniline ring, although the 3′-Br compound **11** has the lowest toxicity. When comparing the halide functionalization in the *para* position, unlike the ferrocenyl β-diketonate compounds **6** and **7**, the 4′-Cl (**13**) and 4′-Br (**14**) β-ketoiminate compounds are nontoxic against all cell lines (IC_{50} > 100 μM) and are up to 18.5 time less toxic than their β-diketonate analogues (**6** *cf.* **13**, see Figure S5). The 4′-F compound **12** is the only *para* substituted β-ketoiminate compound to show moderate cytotoxicity, with values ranging between 43–55 μM, and is up to 2.3 times more cytotoxic than compounds **13** and **14** (MDA-MB-231, $p < 0.05$).

In order to assess the compounds' selectivity towards cancerous cells, the compounds and clinical drugs were screened against normal prostate epithelium cells, PNT2 (Table 2 and Figure 8). Generally, the IC_{50} values show the ferrocenyl β-diketonate compounds **1**–**7** are between 2.2 (**2** *cf.* **9**) and 10.6 times (**4** *cf.* **11**) more potent towards normal cells, than the ferrocenyl β-ketoiminate compounds **8**–**14**. The IC_{50} values of compounds against PNT2 were divided by the IC_{50} values against either of the cancerous cell lines, to give a selectivity index (SI) value. The SI values are shown in parentheses of Table 2 and displayed as a bar-chart in Figure 9. SI values > 1 indicate a selectivity for the cancerous cell line, and highlight the potential to overcome issues of toxicity towards healthy cells. The clinical compound OXA has no selectivity for cancerous cells, with all SI values < 1. However, CDDP shows the highest selectivity, with all SI values between 2.8–5.7, whilst CARB is only selective towards HCT116 $p53^{+/+}$ (SI = 4.5).

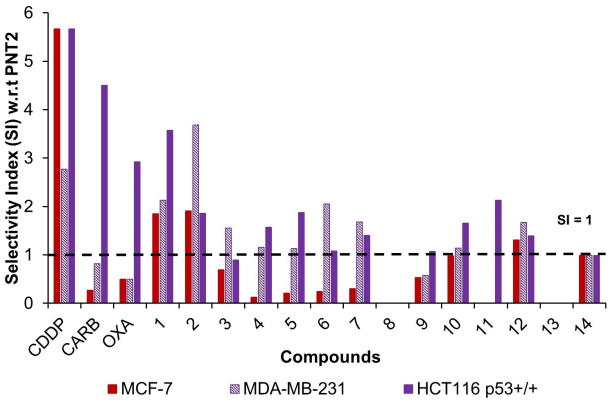

Figure 8. SI values for CDDP, CARB, OXA, and compounds **1**–**14** when comparing the IC_{50} values against cancerous and PNT2. SI > 1 indicates selectivity for the cancer cell lines, SI = 1 indicates equitoxicity for cancerous and normal cell lines, and SI < 1 indicates selectivity for the PNT2.

The ferrocenyl compounds **1**–**14** generally do not have a selectivity towards MCF-7, except for compounds **1** and **2**, which have SI values of 1.9. The compounds have a higher selectivity towards MDA-MB-231 and HCT116 $p53^{+/+}$, with SI values ranging from 0.6–3.7 and 0.9–3.6, respectively. The ferrocenyl β-diketonate compounds **1**–**7** are generally more

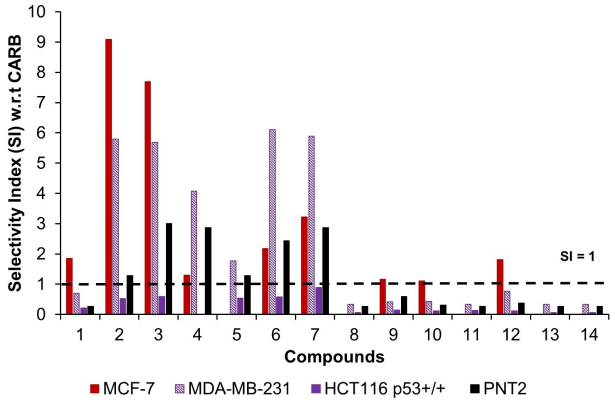

Figure 9. SI values for compounds **1**–**14** when comparing the IC_{50} values with CARB. SI > 1 indicates selectivity for the ferrocenyl compounds, SI = 1 indicates equitoxicity and SI < 1 indicates selectivity for CARB.

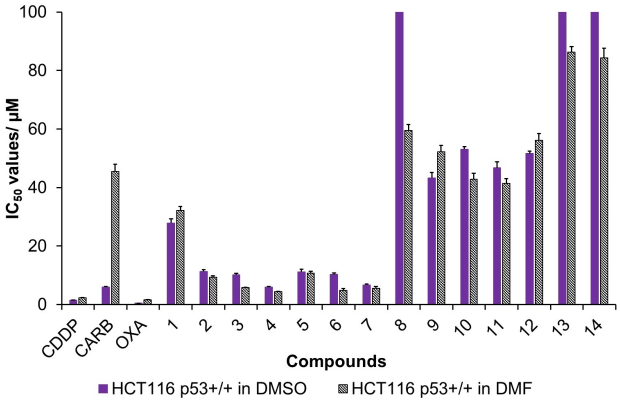

Figure 10. Bar chart of IC_{50} values against HCT116 $p53^{+/+}$ when compounds were dissolved in either DMSO (purple) or DMF (grey)

selective than the analogous ferrocenyl β-ketoiminate compounds **8**–**14**. In particular, compounds **1** and **2** have the highest selectivity against all cell lines. On comparing compounds **1** with **8** (R = H) and **2** with **9** (R = 3′-F), compound **1** is at least 3.6 times more selective than **8** (HCT116 $p53^{+/+}$), whilst **2** is at least 6.4 times more selective than **9** (MDA-MB-231).

The SI values were also calculated for compounds **1**–**14** in comparison with CDDP, CARB and OXA. The results for CDDP and OXA show no selectivity, and these clinical compounds outperform our library or ferrocenyl compounds (Figures S8 and S9). However, compounds **1**–**14** are generally more selective for breast cancer cell lines MCF-7 and MDA-MB-231, when compared to CARB (Figure 9). On comparison of CARB and compounds **2** and **3**, these compounds have increased selectivity against MCF-7, with SI values of 9.1 and 7.8, respectively. Whilst compounds **2**–**7** are all more selective than CARB against MDA-MB-231, with SI values up to 6.1 (**6**). As with the other cytotoxicity results, the ferrocenyl β-diketonate compounds **1**–**7** are generally more selective than ferrocenyl β-ketoiminate compounds **8**–**14** when compared to CARB, with SI values up to 18.5 times higher (**6** *cf.* to **13** against MDA-MB-231).

Due to the differences observed in the NMR spectroscopy of the compounds in [D_6]DMSO and [D_7]DMF (Figures 4 and 5 and S3–S6), and the previously reported cytotoxicity differences observed when iridium compounds were screened in DMSO and DMF,[40] the compounds **1**–**14** were screened against HCT116 $p53^{+/+}$ after being dissolved in DMF. As with the DMSO screening, 100 mM stock solutions of compounds **1**–**14** and the clinical drugs (CDDP, OXA, CARB) were freshly prepared in DMF and immediately (< 5 mins) incubated with cell lines for 96 h (DMF < 0.1% v/v) before performing an MTT assay. The IC_{50} values for CDDP are comparable ($p > 0.05$), however, the values for OXA and CARB significantly decrease in DMF (Table 2 and Figure 10), by 3.6 and 7.6-fold, respectively. On comparison of the IC_{50} values of compounds **1**–**14** in DMSO and DMF, with the exception of compound **8**, where the IC_{50} value increases in DMF (1.6-fold), all compounds have similar activities in both DMSO and DMF, indicating that neither of these solvents has a significant effect on the overall cytotoxicity. Yi and Bae highlighted the decrease in cytotoxicity of the clinical platinum compounds against human ovarian carcinoma (A2780) when changing solvents from DMSO to DMF.[40] Which is contradictory to what was observed by Gasser and co-workers, where the cytotoxicity of iridium compounds and CDDP against A2780 and HeLa generally increased in DMF.[40]

In conclusion, we report the synthesis of seven ferrocenyl β-diketonate compounds (**1**–**7**) and seven ferrocenyl β-ketoiminate compounds (**8**–**14**), including single crystal X-ray analysis of thirteen new compounds. ^{1}H NMR studies were used to assess the compounds' stabilities in [D_6]DMSO and [D_7]DMF, and results indicate no oxidation of the metal center from Fe^{II} to Fe^{III} over a 4 day period, yet there is a possible rearrangement of the compound in solution. Additional mass spectrometry analysis was conducted to understand the possible structure in DMSO and DMF over time, yet no conclusions could be drawn to the species in solution. The library of compounds were screened against human breast carcinoma (MCF-7, MDA-MB-231), human colorectal adenocarcinoma, *p53* wild type (HCT116 $p53^{+/+}$) and normal human prostate cell line (PNT2) cell lines. Generally, the ferrocenyl β-diketonate compounds show a significant increase in cytotoxicity when compared to the analogues ferrocenyl β-ketoiminate compounds. Several compounds are more cytotoxic when compared to CARB, particularly against MCF-7 (SI > 9x) and MDA-MB-231 (SI > 6x). When comparing the results against normal prostate cells, PNT2, the ferrocenyl β-diketonate compounds are less selective than the clinical platinum drugs against MCF-7, however, they exhibit greater selectivity towards MDA-MB-231 and HCT116 $p53^{+/+}$. Additional chemosensitivity studies were conducted after stock solutions were made in DMF. The results highlight only small changes are observed in the compounds potency, whereas the clinical platinum drugs (CDDP, CARB, OXA) in DMF all show varying degrees of lower toxicity when screened against HCT116 $p53^{+/+}$.

Experimental Section

The general experimental details, X-ray crystallography and cell culture protocols can be found in the Supporting Information.

Synthesis of [$C_{14}H_{14}FeO_2$] (1): Acetyl ferrocene (2.80 g, 12.3 mmol) was dissolved in ethyl acetate (25 mL) and stirred before the addition of sodium ethoxide (1.70 g, 25.0 mmol). The solution was stirred at reflux for 3 h forming a yellow solid which was filtered and washed with ethyl acetate. The yellow solid was then dissolved in distilled water (150 mL) and acidified with 10% hydrochloric acid until pH 5 which caused a red solid to precipitate. Recrystallization from hexane gave red crystals (the resonances for enol are stated, however, a small amount of the diketonate resonance form is observed). Yield: 2.70 g, 81%; ^{1}H NMR (500 MHz, $CDCl_3$, δ): 5.63 (s, 1H, methine CH), 4.77 (br. t, 2H, $^3J(^1H\text{-}^1H) = 6.8$ Hz, Cp-CH), 4.50 (d, 2H, $^3J(^1H\text{-}^1H) = 4.1$ Hz, Cp-CH), 4.19 (s, 5H, Cp-C_5H_5), 2.00 (s, 3H, CH_3); $^{13}C\{^1H\}$ NMR (125 MHz, $CDCl_3$, δ): 192.5 (Q, CO), 186.4 (Q, CO), 98.2 (methine CH), 77.7 (Q, Cp), 73.1 (Cp-CH), 72.1 (Cp-CH), 70.3 (Cp-C_5H_5), 70.1 (Cp-CH), 68.7 (Cp-CH), 24.2 (CH_3); Analysis Calculated for $C_{14}H_{14}FeO_2$: C 62.25, H 5.22%, Found: C 62.28, H 5.10%; HRMS [ES^+]: 271.041 [MH^+]

Synthesis of compounds 2–7: Acetyl ferrocene (1 eq.) was dissolved in diethyl ether (20 mL) and with stirring sodium ethoxide (1 eq.) and a functionalized benzoate (1 eq.) were added, and the mixture refluxed for 24 h. The solid precipitate was isolated by filtration, dissolved in distilled water (150 mL) and acidified with 10% hydrochloric acid until pH 5 which caused a red solid to precipitate. The solid was filtered and dried overnight under vacuum before purification.

[$C_{19}H_{15}FFeO_2$] (2): The product was purified by column chromatography, eluting with 83:17 v/v hexane/ethyl acetate to give a red solid. Yield: 2.00 g, 80%; ^{1}H NMR (500 MHz, $(CD_3)_2CO$, δ): 7.77 (br. d, 1H, $^3J(^1H\text{-}^1H) = 7.8$ Hz, phenyl-CH), 7.66 (br. d, 1H, $^3J(^1H\text{-}^1H) = 10.1$ Hz, phenyl-CH), 7.44 (dt, 1H, $^3J(^1H\text{-}^1H) = 8.2$, 6.0 Hz, phenyl-CH), 7.22 (td, 1H, $^3J(^1H\text{-}^1H) = 8.4$ and $^4J(^1H\text{-}^1H) = 1.8$ Hz, phenyl CH), 6.68 (s, 1H, methine CH), 4.95 (br. s, 2H, Cp-CH), 4.52 (br. s, 2H, Cp-CH), 4.11 (s, 5H, Cp-C_5H_5); $^{13}C\{^1H\}$ NMR (125 MHz, $(CD_3)_2CO$, δ): 196.0 (Q, CO), 178.37 (Q, CO), 163.9 (d, Q, CF, $^1J(^{13}C\text{-}^{19}F) = 243.9$ Hz), 138.6 (d, Q phenyl-C, $^3J(^{13}C\text{-}^{19}F) = 7.8$ Hz), 131.5 (d, phenyl-CH, $^3J(^{13}C\text{-}^{19}F) = 8.3$ Hz), 123.6 (d, phenyl-CH, $^4J(^{13}C\text{-}^{19}F) = 2.1$ Hz), 119.4 (d„ phenyl-CH, $^2J(^{13}C\text{-}^{19}F) = 21.8$ Hz,), 114.2 (d„ phenyl-CH, $^2J(^{13}C\text{-}^{19}F) = 23.9$ Hz), 95.1 (methine CH), 79.0 (Q, Cp), 73.5 (Cp-CH), 71.2 (Cp-C_5H_5), 69.9 (Cp-CH); Analysis Calculatedfor $C_{19}H_{15}FFeO_2$: C 65.17, H 4.32%, Found C 65.10, H 4.30%; HRMS [ES^+]: 349.032 [$M-H^+$]

[$C_{19}H_{15}ClFeO_2$] (3): The product was purified by column chromatography, eluting with 90:10 v/v hexane/ethyl acetate to give a red solid. Yield: 1.89 g, 72%; ^{1}H NMR (500 MHz, $(CD_3)_2CO$, δ): 7.92 (t, 1H, $^4J(^1H\text{-}^1H) = 1.8$ Hz, phenyl-CH), 7.88 (dt, 1H, $^3J(^1H\text{-}^1H) = 7.8$ and $^4J(^1H\text{-}^1H) = 1.3$ Hz, phenyl-CH), 7.48 (dq, 1H, $^3J(^1H\text{-}^1H) = 7.8$ and $^4J(^1H\text{-}^1H) = 1.0$ Hz, phenyl-CH), 7.42 (t, 1H, $^3J(^1H\text{-}^1H) = 7.8$ Hz, phenyl-CH), 6.70 (s, 1H, methane CH), 4.95 (t, 2H, $^3J(^1H\text{-}^1H) = 2.0$ Hz, Cp-CH), 4.52 (t, 2H, $^3J(^1H\text{-}^1H) = 2.0$ Hz, Cp-CH), 4.12 (s, 5H, Cp-C_5H_5); $^{13}C\{^1H\}$ NMR (125 MHz, $(CD_3)_2CO$, δ): 196.0 (Q, CO), 178.3 (Q, CO), 138.2 (Q, phenyl-C), 135.2 (Q, C–Cl), 132.4 (phenyl-CH), 131.3 (phenyl-CH), 127.4 (phenyl-CH), 126.1 (phenyl-CH), 95.1 (methine CH), 79.0 (Q, Cp), 73.5 (Cp-CH), 71.2 (Cp-C_5H_5), 69.9 (Cp-CH); Analysis Calculated for $C_{19}H_{15}ClFeO_2$: C 62.25, H 4.12%, Found: C 62.18, H 4.13%; HRMS [ES^+]: 366.010 [MH^+]

[$C_{19}H_{15}BrFeO_2$] (4): The product was purified by column chromatography, eluting with 90:10 v/v hexane/ethyl acetate to give a red solid. Yield: 2.32 g, 78%; ^{1}H NMR (500 MHz, $(CD_3)_2CO$, δ): 8.07 (t, 1H, $^4J(^1H\text{-}^1H) = 1.6$ Hz, phenyl-CH), 7.93 (dt, 1H, $^3J(^1H\text{-}^1H) = 7.8$ and $^4J(^1H\text{-}^1H) = 1.1$ Hz, phenyl-CH), 7.62 (dt, 1H, $^3J(^1H\text{-}^1H) = 8.0$ and $^4J(^1H\text{-}^1H) = 0.8$ Hz, phenyl-CH), 7.36 (t, 1H, $^3J(^1H\text{-}^1H) = 7.9$ Hz, phenyl-CH), 6.69 (s, 1H, methine CH), 4.94 (t, 2H, $^3J(^1H\text{-}^1H) = 1.8$ Hz, Cp-CH), 4.52 (t, 2H, $^3J(^1H\text{-}^1H) = 1.8$ Hz, Cp-CH), 4.11 (s, 5H, Cp-C_5H_5); $^{13}C\{^1H\}$ NMR (125 MHz, $(CD_3)_2CO$, δ): 196.0 (Q, CO), 178.3 (Q, CO), 138.4 (Q, phenyl-C), 135.4 (phenyl-CH), 131.5 (phenyl-CH), 130.3 (phenyl-CH), 126.5 (phenyl-CH), 123.3 (Q, C-Br), 95.1 (methine CH), 79.0 (Q, Cp), 73.5 (Cp-CH), 71.2 (Cp-C_5H5), 69.9 (Cp-CH); Analysis Calculated for $C_{19}H_{15}BrFeO$: C 55.52, H 3.68%, Found: C 55.54, H 3.77%; HRMS [ES^+]: 409.960 [MH^+]

[$C_{19}H_{15}FFeO_2$] (5): The product was purified by column chromatography, eluting with 80:20 v/v hexane/ethyl acetate to give a red solid. Yield: 1.59 g, 63%; ^{1}H NMR (500 MHz, $(CD_3)_2CO$, δ): 8.10 (m, 2H, phenyl-CH), 7.29 (t, 2H, $^3J(^1H\text{-}^1H) = 8.7$ Hz, phenyl-CH), 6.59 (s, 1H, methine CH), 5.00 (t, 2H, $^3J(^1H\text{-}^1H) = 1.8$ Hz, Cp-CH), 4.66 (t, 2H, $^3J(^1H\text{-}^1H) = 1.8$ Hz, Cp-CH), 4.26 (s, 5H, Cp-C_5H_5); $^{13}C\{^1H\}$ (125 MHz, $(CD_3)_2CO$, δ): 195.0 (Q, CO), 179.7 (Q, CO), 165.8 (d, Q, C-F, $^1J(^{13}C\text{-}^{19}F) = 250.2$ Hz), 132.6 (d, Q, phenyl-C, $^4J(^{13}C\text{-}^{19}F) = 2.1$ Hz), 130.3 (d, phenyl-CH, $^3J(^{13}C\text{-}^{19}F) = 9.3$ Hz), 116.4 (d, phenyl-CH, $^2J(^{13}C\text{-}^{19}F) = 21.8$ Hz), 94.4 (methine CH), 73.5 (Q, Cp), 73.2 (Cp-CH), 71.1 (Cp-C_5H_5), 70.8 (Cp-CH), 70.6 (Cp-CH), 69.8 (Cp-CH); Analysis Calculated for $C_{19}H_{15}FFeO_2$: C 65.17, H 4.32%, Found: C 65.00, H 4.40%; HRMS [ES^+]: 349.330 [$M-H^+$]

[$C_{19}H_{15}ClFeO_2$] (6): The product was purified by column chromatography, eluting with 83:17 v/v hexane/ethyl acetate to give a red solid. Yield: 1.65 g, 63%; ^{1}H NMR (500 MHz, $(CD_3)_2CO$, δ): 7.95 (d, 2H, $^3J(^1H\text{-}^1H) = 8.7$ Hz, phenyl-CH), 7.41 (d, 2H, $^3J(^1H\text{-}^1H) = 8.7$ Hz, phenyl-CH), 6.36 (d, 1H, $^3J(^1H\text{-}^1H) = 5.5$ Hz, methine CH), 4.92 (br. t, 2H, $^3J(^1H\text{-}^1H) = 1.7$ Hz, Cp-CH), 4.51 (br. t, 2H, $^3J(^1H\text{-}^1H) = 1.7$ Hz, Cp-CH), 4.11 (s, 5H, Cp-C_5H_5); $^{13}C\{^1H\}$ NMR (125 MHz, $(CD_3)_2CO$, δ): 195.7 (Q, CO), 178.9 (Q, CO), 134.9 (Q, phenyl-C), 131.4 (Q, C-Cl), 129.7 (phenyl-CH), 129.3 (phenyl-CH), 94.8 (methine CH), 79.1 (Q, Cp), 73.4 (Cp-CH), 71.2 (Cp-C_5H_5), 69.8 (Cp-CH); Analysis Calculated for $C_{19}H_{15}ClFeO_2$: C 62.25, H 4.12, Cl 9.67%, Found: C 62.30, H 4.10, Cl 9.50%; HRMS [ES^+]: 366.011 [MH^+]

[$C_{19}H_{15}BrFeO_2$] (7): The product was purified by column chromatography, eluting with 90:10 v/v hexane/ethyl acetate to give a red solid. Yield: 2.76 g, 93%; ^{1}H NMR (500 MHz, $(CD_3)_2CO$, δ): 7.87 (d, 2H, $^3J(^1H\text{-}^1H) = 8.0$ Hz, phenyl-CH), 7.58 (d, 2H, $^3J(^1H\text{-}^1H) = 7.1$ Hz, phenyl-CH), 6.66 (s, 1H, methine CH), 4.92 (br. s, 2H, Cp-CH), 4.51 (br. s, 2H, Cp-CH), 4.11 (s, 5H, Cp-C_5H_5); $^{13}C\{^1H\}$ NMR (125 MHz, $CDCl_3$, δ): 194.3 (Q, CO), 178.5 (Q, CO), 134.2 (Q, phenyl-C), 131.9 (phenyl-CH), 128.2 (phenyl-CH), 126.5 (Q, C-Br), 93.6 (methine CH), 78.0 (Q, Cp), 72.4 (Cp-CH), 70.4 (Cp-C_5H_5), 68.8 (Cp-CH); Analysis Calculated for $C_{19}H_{15}BrFeO_2$ (+0.75 DCM): C 49.96, H 3.50%, Found: C 50.00, H 3.20%; HRMS [ES^+]: 409.960 [MH^+]

Synthesis of complexes 8–14: 1-Ferrocenylbutane-1,3-dione (compound **1**, 1 eq.) was dissolved in ethanol (20 mL) followed by the addition of a functionalized aniline (2 eq.) and concentrated hydrochloric acid (2 mL). The reaction was stirred at room temperature for 3 days. The solution was filtered and the solvent removed *in vacuo*.

[$C_{20}H_{19}FeNO$] (8): The crude solid was dissolved in ethyl acetate/hexane (1:4) and filtered through a silica plug. The solvent was removed, leaving a red solid. Red crystals were obtained upon slow evaporation from acetone. Yield: 0.86 g, 68%; ^{1}H NMR (300 MHz, $(CD_3)_2CO$, δ): 12.86 (s, 1H, NH), 7.50–7.34 (m, 2H, phenyl-CH), 7.31–7.14 (m, 3H, phenyl-CH), 5.65 (s, 1H, methine CH), 4.86–4.75 (m, 2H, m, Cp-CH), 4.47–4.37 (m, 2H, Cp-CH), 4.17 (s, 5H, Cp-C_5H_5), 2.16 (s, 3H, CH_3); $^{13}C\{^1H\}$ NMR (101 MHz, $(CD_3)_2CO$, δ): 193.00 (Q, CO), 159.15 (Q, phenyl-C), 139.32 (Q, CNH), 129.22 (phenyl-CH), 125.18 (phenyl-CH), 124.33 (phenyl-CH), 95.68 (methine CH), 82.45 (Q, Cp), 71.05 (Cp-CH), 69.94 (Cp-C_5H_5), 68.60 (Cp-CH), 20.58 (CH_3). HRMS [ES^+]: 346.0915 [$M-H^+$] (calculated 346.0889)

[$C_{20}H_{18}FFeNO$] (9): The crude solid was dissolved in ethyl acetate/hexane (3:7) and filtered through a silica plug. The solvent was removed, and the crude product was dissolved in an ethanol/ether mixture, and cooled to −20 °C overnight, yielding red crystals. Yield: 0.49 g, 40%; ^{1}H NMR (300 MHz, $(CD_3)_2CO$, δ): 12.89 (s, 1H, NH), 7.42(m, 1H, phenyl-CH), 7.07 (m, 2H, phenyl-CH) 6.94 (m, 1H, phenyl-CH), 5.69 (s, 1H, methine CH), 4.85–4.77 (m, 2H, Cp-CH), 4.49–4.40 (m, 2 H, Cp-CH), 4.17 (s, 5H, Cp-C_5H_5), 2.22 (s, 3H, CH_3); ^{13}C{^{1}H} NMR (101 MHz, $(CD_3)_2CO$, δ): 192.81 (Q, CO), 157.80 (Q, phenyl-C), 142.51 (Q, CNH), 139.24 (phenyl-CH), 130.72 (phenyl-CH), 119.08 (Q, C-FI), 110.92 (phenyl-CH), 110.10 (phenyl-CH), 96.56 (methine CH), 83.67 (Q, Cp), 70.87 (Cp-CH), 70.27 (Cp-C_5H_5), 69.50 (Cp-CH), 19.56 (CH_3); HRMS [ES$^+$]: 364.0845 [M−H$^+$]

[$C_{20}H_{18}ClFeNO$] (10): The crude solid was dissolved in ethyl acetate/hexane (1:4) and filtered through a silica plug. The solvent was removed, leaving a red solid. Red crystals were obtained upon slow evaporation from acetone. **Yield**: 0.82 g, 58%; 1H NMR (300 MHz, $(CD_3)_2CO$, δ): 12.87 (s, 1H, NH), 7.46–7.34 (m, 1H, phenyl-CH), 7.29 (t, 1H, ^4J(^{1}H-^{1}H) = 2.0, phenyl-CH), 7.20 (dd, 2H, ^3J(^{1}H-^{1}H) = 7.9 and ^4J (^{1}H-^{1}H) = 1.9, phenyl-CH), 5.69 (s, 1H, methine CH), 4.81 (s, 2H, Cp-CH), 4.43 (s, 2H, Cp-CH), 4.17 (s, 5H, Cp-C_5H_5), 2.21 (s, 3H, CH_3); ^{13}C {^{1}H} NMR (100 MHz, $(CD_3)_2CO$, δ): 192.85 (Q, CO), 157.80 (Q, phenyl-C), 141.17 (Q, CNH), 134.21 (phenyl-CH), 130.58 (phenyl-CH), 124.23 (phenyl-CH), 123.02 (phenyl-CH), 121.78 phenyl-CH), 96.61 (methine CH), 82.38 (Q, Cp), 70.90 (Cp-CH), 69.63 (Cp-C_5H_5), 68.51 (Cp-CH), 19.51 (CH_3); Analysis Calculated for $C_{20}H_{18}ClFeNO$: C 63.27 H 4.78 N 3.69 Cl 9.34%; Found: C 62.90 H 4.80 N 3.50 Cl 9.10%; HRMS [ES$^+$]: 380.0507 [M + H]$^+$

[$C_{20}H_{18}BrFeNO$] (11): The crude solid was dissolved in ethyl acetate/hexane (1:4) and filtered through a silica plug. The solvent was removed, leaving a red solid. Red crystals were obtained upon slow evaporation from acetone. **Yield**: 0.62 g, 39%; ^{1}H NMR (300 MHz, $(CD_3)_2CO$, δ): 12.86 (s, 1H, NH), 7.44 (br. t, 1H, phenyl-CH), 7.39–7.18 (m, 2H, phenyl-CH), 7.29–7.21 (m, 1H, phenyl-CH), 5.69 (s, 1H, methine CH), 4.85–4.77 (m, 2H, Cp-CH), 4.48–4.40 (m, 2H, Cp-CH), 4.17 (s, 5H, Cp-C_5H_5), 2.20 (s, 3H, CH_3); ^{13}C{^{1}H} NMR (100 MHz, $(CD_3)_2CO$, δ) 192.83 (Q, CO), 157.76 (Q, phenyl-C), 157.37 (Q, CNH), 141.31 (phenyl-CH), 130.83 (phenyl-CH), 127.21 (phenyl-CH), 125.94 (phenyl-CH), 122.22 (phenyl-CH), 96.62 (methine CH), 82.39 (Cp-CH), 70.89 (Cp-CH), 70.06 (Cp-C_5H_5), 69.63 (Cp-CH), 19.48 (CH_3); Analysis Calculated for $C_{20}H_{18}BrFeNO$: C 56.64 H 4.28 N 3.30%; Found: C 56.10 H 4.30 N 3.00%; HRMS [ES$^+$]: 425.9996 [M + H]$^+$

[$C_{20}H_{18}FFeNO$] (12): After addition of HCl, the reaction was heated to 80 °C and stirred overnight. The solution was filtered and the remaining solid washed with toluene and petroleum ether. The solvent was removed, leaving a red-brown oil, before being purified by column chromatography, eluting with 80:20 dichloromethane/petroleum ether to give an orange solid. Yield: 0.49 g, 34%; ^{1}H (300 MHz, $(CD_3)_2CO$, δ): 12.73 (s, 1H, NH), 7.29 (dd, 2H, ^3J(^{1}H-^{1}H) = 9.0 and ^4J(^{1}H-^{1}H) = 4.9, phenyl-CH), 7.23 (br. tt, 2H, phenyl-CH), 5.65 (s, 1H, methine CH), 4.79 (t, 2H, ^4J(^{1}H-^{1}H) = 1.9, Cp-CH), 4.41 (t, 2H, ^4J (^{1}H-^{1}H) = 1.9, Cp-CH), 4.16 (s, 5H, Cp-C_5H_5), 2.10 (s, 3H, CH_3); ^{13}C{^{1}H} NMR (500 MHz, $(CD_3)_2CO$, δ) 193.3 (Q, CO), 162.0 (Q, C-Cl), 159.8 (phenyl-CH), 136.6 (Q, CNH), 126.9 (phenyl-CH), 116.6 (phenyl-CH), 96.3 (methine CH), 83.6 (Cp-CH), 72.8 (Cp-CH), 70.9 (Cp-C_5H_5), 69.4 (Cp-CH), 20.1 (CH_3); Analysis Calculated for $C_{20}H_{18}FFeNO$: C 67.65, H 5.00, N 3.86%; Found: C 64.90, H 5.10, N 5.70%; HRMS [ES$^+$]: 364.0798 [M + H]$^+$

[$C_{20}H_{18}ClFeNO$] (13): The reaction mixture was stirred at room temperature overnight. TLC showed the presence of 1-ferrocenyl-butane-1,3-dione but no aniline. A further 0.93 g (7.4 mmol) of 4-chloroaniline was added and the reaction mixture stirred for another 2 days. The solvent was removed *in vacuo* and the resulting solid purified by column chromatography, eluting with ethyl acetate/hexane (1:9). The resulting solid was recrystallized from hot ethanol, giving red crystals. Yield: 0.69 g, 49%; ^{1}H (300 MHz, $(CD_3)_2CO$, δ): 12.87 (s, 1H, NH), 7.45 (d, 2H, ^3J(^{1}H-^{1}H) = 8.8, phenyl-CH), 7.30 (d, 2H, ^3J(^{1}H-^{1}H) = 8.8, phenyl-CH), 5.71 (s, 1H, methine CH), 4.90–4.80 (m, 2H, Cp-CH), 4.52–4.42 (m, 2H, Cp-CH), 4.20 (s, 5H, Cp-C_5H_5), 2.21 (s, 3H, CH_3); ^{13}C{^{1}H} NMR (100 MHz, $(CD_3)_2CO$, δ): 193.54 (Q, CO), 159.00 (Q, CNH), 139.42 (Q, phenyl-C), 130.04 (phenyl-CH), 125.94 (phenyl-CH), 97.09 (methine CH), 83.41 (Q, Cp), 71.70 (Cp-CH), 70.50 (Cp-C_5H_5), 69.36 (Cp-CH), 20.30 (CH_3). Analysis Calculated for $C_{20}H_{18}ClFeNO$: C 63.27, H 4.78, N 3.69, Cl 9.34%, Found: C 63.00, H 4.90, N 3.40, Cl 9.25%. HRMS [ES$^+$]: 380.0510 [M−H$^+$]

[$C_{20}H_{18}ClFeNO$] (14): The crude solid was dissolved in ethyl acetate/hexane (1:4), and filtered through a silica plug. The solvent was removed and the red solid recrystallized from hot ethanol yielding red crystals. Yield: 0.72 g, 46%; ^{1}H (300 MHz, $(CD_3)_2CO$, δ): 12.83 (s, 1H, NH), 7.55 ('d, 2H, ^3J(^{1}H-^{1}H) = 8.8, phenyl-CH), 7.21 (d, 2H, ^3J (^{1}H-^{1}H) = 8.8, phenyl-CH), 5.68 (s, 1H, methine CH), 4.84–4.76 (m, 2H, Cp-CH), 4.47–4.39 (m, 2H, Cp-CH), 4.17 (s, 5H, Cp-C_5H_5), 2.18 (s, 3H, CH_3); ^{13}C{^{1}H} NMR (300 MHz, [D_6]DMSO, δ): 192.72 (Q, CO), 158.51 (Q, CNH), 138.80 (Q, phenyl-C), 132.50 (phenyl-CH), 125.65 (phenyl-CH), 117.16 (phenyl-CH), 96.73 (methine CH), 82.52 (Q, Cp), 71.39 (Cp-CH), 70.02 (Cp-C_5H_5), 68.82 (Cp-CH), 20.41 (CH_3); Analysis Calculated for $C_{20}H_{18}ClFeNO$: C 56.64, H 4.28, N 3.30, Br 18.84%, Found: C 56.50, H 4.35, N 3.10, Br 18.70%. HRMS [ES$^+$]: 425.999 [M−H$^+$]

Acknowledgements

We would like to thank the University of Leeds, University of Bradford and University of East Anglia, for their support in this publication. In particular, we thank Tanya Marinko-Covell (University of Leeds) and Stephen Boyer (London Metropolitan University) for elemental analysis, and Dr. Markus Zegke (Universität zu Köln) for X-ray crystallographic discussions, Dr Alex Surtees (University of Bradford) for NMR assistnace and Dr Pablo Caramés Méndez (University of Leeds) for mass spectrometry assistance. A special thank you to the Institute of Cancer Therapeutics (University of Bradford) for providing cell lines and cell culture facilities.

Conflict of Interest

The authors declare no conflict of interest.

Keywords: β-diketonate ligands · β-ketoiminate ligands · bioinorganic chemistry · cancer · ferrocenyl compounds

[1] B. Rosenberg, L. Van Camp, T. Krigas, *Nature* **1965**, *205*, 698–699.
[2] A. Bergamo, R. Gagliardi, V. Scarcia, A. Furlani, E. Alessio, G. Mestroni, G. Sava, *J. Pharmacol. Exp. Ther.* **1999**, *289*, 559–564.
[3] S. Dasari, P. B. Tchounwou, *Eur. J. Pharmacol.* **2014**, *740*, 364–378.
[4] P. Comella, R. Casaretti, C. Sandomenico, A. Avallone, L. Franco, *Ther. Clin. Risk Manage.* **2009**, *5*, 229–238.
[5] D. J. Stewart, *Crit. Rev. Oncol. Hematol.* **2007**, *63*, 12–31.
[6] J. T. Hartmann, H.-P. Lipp, *Expert Opin. Pharmacother.* **2003**, *4*, 889–901.
[7] M. J. Clarke, F. Zhu, D. R. Frasca, *Chem. Rev.* **1999**, *99*, 2511–2534.
[8] P. Köpf-Maier, *Eur. J. Clin. Pharmacol.* **1994**, *47*, 1–16.
[9] A. M. Evangelou, *Crit. Rev. Oncol. Hematol.* **2002**, *42*, 249–265.

[10] C.-H. Leung, H.-J. Zhong, D. S.-H. Chan, D.-L. Ma, *Coord. Chem. Rev.* **2013**, *257*, 1764–1776.
[11] B. Bertrand, A. Casini, *Dalton Trans.* **2014**, *43*, 4209–4219.
[12] S. Top, A. Vessières, C. Cabestaing, I. Laios, G. Leclercq, C. Provot, G. Jaouen, *J. Organomet. Chem.* **2001**, *637–639*, 500–506.
[13] S. Top, A. Vessières, P. Pigeon, M.-N. Rager, M. Huché, E. Salomon, C. Cabestaing, J. Vaissermann, G. Jaouen, *ChemBioChem* n.d., *5*, 1104–1113.
[14] S. Top, J. Tang, A. Vessières, D. Carrez, C. Provot, G. Jaouen, *Chem. Commun.* **1996**, *0*, 955–956.
[15] E. Allard, C. Passirani, E. Garcion, P. Pigeon, A. Vessières, G. Jaouen, J.-P. Benoit, *J. Controlled Release* **2008**, *130*, 146–153.
[16] E. Allard, N. T. Huynh, A. Vessières, P. Pigeon, G. Jaouen, J.-P. Benoit, C. Passirani, *Int. J. Pharm.* **2009**, *379*, 317–323.
[17] G. Jaouen, A. Vessières, S. Top, *Chem. Soc. Rev.* **2015**, *44*, 8802–8817.
[18] H. Tamura, M. Miwa, *Chem. Lett.* **1997**, *26*, 1177–1178.
[19] S. Sansook, E. Lineham, S. Hassell-Hart, G. J. Tizzard, S. J. Coles, J. Spencer, S. J. Morley, *Molecules.* **2018**, *23*, 2126.
[20] S. Peter, B. A. Aderibigbe, *Molecules* **2019**, *24*, 3604.
[21] G. Gasser, I. Ott, N. Metzler-Nolte, *J. Med. Chem.* **2011**, *54*, 3–25.
[22] J. Hess, J. Keiser, G. Gasser, *Future Med. Chem.* **2015**, *7*, 821–830.
[23] A. Vessières, C. Corbet, J. M. Heldt, N. Lories, N. Jouy, I. Laïos, G. Leclercq, G. Jaouen, R.-A. Toillon, *J. Inorg. Biochem.* **2010**, *104*, 503–511.
[24] R. Epton, M. E. Hobson, G. Marr, *J. Organomet. Chem.* **1978**, *149*, 231–244.
[25] J. R. Pladziewicz, M. J. Carney, *J. Am. Chem. Soc.* **1982**, *104*, 3544–3545.
[26] J. R. Pladziewicz, A. J. Abrahamson, R. A. Davis, M. D. Likar, *Inorg. Chem.* **1987**, *26*, 2058–2062.
[27] D. Hamels, P. M. Dansette, E. A. Hillard, S. Top, A. Vessières, P. Herson, G. Jaouen, D. Mansuy, *Angew. Chem. Int. Ed.* **2009**, *48*, 9124–9126; *Angew. Chem.* **2009**, *121*, 9288–9290.
[28] A. Citta, A. Folda, A. Bindoli, P. Pigeon, S. Top, A. Vessières, M. Salmain, G. Jaouen, M. P. Rigobello, *J. Med. Chem.* **2014**, *57*, 8849–8859.
[29] V. Scalcon, M. Salmain, A. Folda, S. Top, P. Pigeon, H. Z. S. Lee, G. Jaouen, A. Bindoli, A. Vessières, M. P. Rigobello, *Metallomics* **2017**, *9*, 949–959.
[30] J. C. Swarts, T. G. Vosloo, S. J. Cronje, W. C. Du Plessis, C. E. J. Van Rensburg, E. Kreft, J. E. Van Lier, *Anticancer Res.* **2008**, *28*, 2781–2784.
[31] R. M. Lord, J. J. Mannion, A. J. Hebden, A. E. Nako, B. D. Crossley, M. W. McMullon, F. D. Janeway, R. M. Phillips, P. C. McGowan, *ChemMedChem* **2014**, *9*, 1136–1139.
[32] R. M. Lord, A. J. Hebden, C. M. Pask, I. R. Henderson, S. J. Allison, S. L. Shepherd, R. M. Phillips, P. C. McGowan, *J. Med. Chem.* **2015**, *58*, 4940–4953.
[33] R. M. Lord, J. J. Mannion, B. D. Crossley, A. J. Hebden, McMullon, J. Fisher, R. M. Phillips, P. C. McGowan, *ChemistrySelect* **2016**, *1*, 6598–6605.
[34] C. Valdebenito, M. T. Garland, M. Fuentealba, A. H. Klahn, C. Manzur, *Acta Crystallogr. Sect. E* **2010**, *E66*, m1655.
[35] F. Wang, S. Islam, V. Vasilyev, *Mater. Basel Switz.* **2015**, *8*, 7723–7737.
[36] J. D. Bourke, M. T. Islam, S. P. Best, C. Q. Tran, F. Wang, C. T. Chantler, *J. Phys. Chem. Lett.* **2016**, *7*, 2792–2796.
[37] G. Alagona, C. Ghio, *Int. J. Quantum Chem.* **2008**, *108*, 1840–1855.
[38] T. Tsukahara, K. Nagaoka, K. Morikawa, K. Mawatari, T. Kitamori, *J. Phys. Chem. B* **2015**, *119*, 14750–14755.
[39] A. Matwijczuk, D. Karcz, R. Walkowiak, J. Furso, B. Gładyszewska, S. Wybraniec, A. Niewiadomy, G. P. Karwasz, M. Gagoś, *J. Phys. Chem. A* **2017**, *121*, 1402–1411.
[40] H. Huang, N. Humbert, V. Bizet, M. Patra, H. Chao, C. Mazet, G. Gasser, *J. Organomet. Chem.* **2017**, *839*, 15–18.

Manuscript received: January 20, 2020
Revised manuscript received: February 23, 2020
Accepted manuscript online: March 16, 2020
Version of record online: April 2, 2020